Electroconvulsive seizure and VEGF increase the proliferation of neural stem-like cells in rat hippocampus

Eri Segi-Nishida, Jennifer L. Warner-Schmidt, and Ronald S. Duman*

Laboratory of Molecular Psychiatry, Department of Psychiatry and Pharmacology, Yale University School of Medicine, New Haven, CT 06508

Edited by Fred H. Gage, Salk Institute for Biological Studies, San Diego, CA, and approved May 7, 2008 (received for review November 15, 2007)

All classes of antidepressants increase hippocampal cell proliferation and neurogenesis, which contributes, in part, to the behavioral actions of these treatments. Among antidepressant treatments, electroconvulsive seizure (ECS) is the most robust stimulator of hippocampal cell proliferation and the most efficacious treatment for depression, but the cellular mechanisms underlying the actions of ECS are unknown. To address this question, we investigated the effect of ECS on proliferation of neural stem-like and/or progenitor cells in the subgranular zone of rat dentate gyrus. We define the neural differentiation cascade from stem-like cells to early neural progenitors (also referred to as quiescent and amplifying neural progenitors, respectively) by coexpression of selective cellular and mitotic activity markers. We find that at an early mitotic phase ECS increases the proliferation of quiescent progenitors and then at a later phase increases the proliferation of amplifying progenitors. We further demonstrate that vascular endothelial growth factor (VEGF) signaling is necessary for ECS induction of quiescent neural progenitor cell proliferation and is sufficient to produce this effect. These findings demonstrate that ECS and subsequent induction of VEGF stimulates the proliferation of neural stem-like cells and neural progenitor cells, thereby accounting for the superior neurogenic actions of ECS compared with chemical antidepressants.

depression | neurogenesis | antidepressant | neurotrophic factor

Electroconvulsive seizure (ECS) therapy is considered the most effective treatment for depression, including patients who do not respond to chemical antidepressants (1–3). Recent studies demonstrate that all classes of antidepressants increase neurogenesis in the adult hippocampus, and this effect is thought to contribute, in part, to the actions of these treatments in rodent behavioral models (4–6). However, the cellular basis for the antidepressant induction of hippocampal neurogenesis has not been fully characterized. Previous studies have demonstrated that antidepressants, such as ECS and fluoxetine, increase cell proliferation within the subgranular zone (SGZ) and accelerate the maturation of immature neuron of the dentate gyrus in hippocampus but do not affect the differentiation of progenitor cells into neurons or glia (7–10). This indicates that one of the main targets for antidepressant-induced neurogenesis is to increase the mitotic activity of neural progenitor cells in the SGZ.

Two major subclasses of proliferating cells have been characterized in the hippocampal SGZ based on the expression of phenotypic marker proteins. The first class is the putative stem cell that has a radial glia-like morphology, characterized by expression of glial fibrillary acidic protein (GFAP) and a relatively low rate of proliferative activity. This cell population is called the neural stem-like cell, type 1 cell, B cell, or quiescent neural progenitor (QNP) (11–13). The second class of cells is GFAP-negative, has a relatively higher rate of mitotic activity, and is referred to as early neural progenitor, type 2a, D cell, or amplifying neural progenitor (ANP) (12, 13). ANP and QNP cells in the SGZ, also express the transcription factor Sox-2, which is considered a marker for identifying both neural stem-like and progenitor cells in neurogenic regions (14–16).

A recent study has reported that chronic administration of a selective serotonin reuptake inhibitor (SSRI), fluoxetine, increases the symmetric division of ANPs in mouse hippocampus without affecting QNPs (13). Although ECS is a far more efficacious stimulator of hippocampal cell proliferation compared with chemical antidepressant treatments (7), the cellular mechanisms underlying the actions of ECS have not been determined. To address this issue, we investigated the effects of ECS on the proliferation of QNP and ANP cell subclasses in SGZ of rat hippocampus. We also examine the role of vascular endothelial growth factor (VEGF) based on our recent report that antidepressant induction of hippocampal cell proliferation requires VEGF signaling (17). We find that ECS increases QNP proliferation at an early mitotic phase and subsequently increases ANP cell proliferation and that VEGF signaling underlies ECS-induced proliferation of both cell subclasses. This induction of neural stem-like cell proliferation by ECS and VEGF signaling explains the superior efficacy of ECS stimulation of hippocampal cell proliferation and subsequent neurogenesis.

Results

Phenotype of BrdU-Labeled QNP and ANP Cells in Rat Hippocampal SGZ. To characterize the proliferating cell types present in SGZ, we examined the expression of Sox-2 and GFAP in BrdU-labeled cells. Sox-2 is a marker for both QNP and ANP cells, and GFAP is a specific marker for QNP cells in the SGZ. Cell phenotypic markers were analyzed 2 h after BrdU injections to characterize cells showing mitotic activity. Most $BrdU^+$ cells within SGZ were also $Sox\text{-}2^+$ in normal animals, indicating that most mitotic cells in SGZ are QNP or ANP cells (>90% of $BrdU^+$ cells; data not shown). We further subdivided these proliferating cells into $BrdU^+$, $Sox\text{-}2^+$, and $GFAP^+$ triple-labeled cells (designated $BrdU^+$QNP), and $BrdU^+$, $Sox\text{-}2^+$ double-labeled cells, but GFAP-negative (designated $BrdU^+$ANP) (Fig. 1).

Confocal analysis and Z-sectioning demonstrate that many $BrdU^+$QNPs have a major process, visualized with GFAP labeling that surrounds the cell body and extends across the granule cell layer [Fig. 1 *A* and *C*; also see supporting information (SI) Fig. S1]. Among total QNPs within SGZ, only 10% of cells were $BrdU^+$, suggesting low mitotic activity of this subclass (Fig. 1*C* and Fig. S2*A*). Although astrocytes also show $Sox\text{-}2^+$ and $GFAP^+$ immunostaining (14), these cells exhibit a stellate morphology and are primarily localized in the hilus (Fig. 1*A*). We also observed

Author contributions: E.S.-N. and R.S.D. designed research; E.S.-N. and J.L.W.-S. performed research; E.S.-N. analyzed data; and E.S.-N. and R.S.D. wrote the paper.

The authors declare no conflict of interest.

This article is a PNAS Direct Submission.

*To whom correspondence should be addressed. E-mail: ronald.duman@yale.edu.

This article contains supporting information online at www.pnas.org/cgi/content/full/0710858105/DCSupplemental.

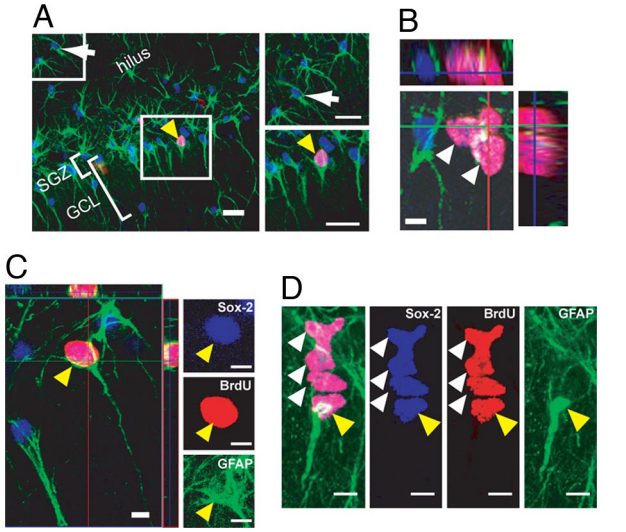

Fig. 1. Analysis of dividing cells using markers for QNPs and ANPs in rat SGZ. Staining for Sox-2 (blue) is used as a marker for both QNPs and ANPs. Staining for GFAP (green) is used as a marker for QNPs. Staining for BrdU (red) is used to measure mitotic activity. (*A*) Confocal micrographs of BrdU-labeled Sox-2$^+$ and GFAP$^+$ QNPs (BrdU$^+$QNP) in rat SGZ 2 h after BrdU injection (yellow arrowheads). (*Left*) Low magnification photomicrograph of hilus and SGZ, which borders the hilus and the granule cell layer (GCL). Among QNPs within SGZ, only a few cells were BrdU$^+$ (indicated by arrowhead). Astrocytes also show Sox-2$^+$ and GFAP$^+$ immunostaining, but most astrocytes in hilus exhibit stellate morphology (white arrows). (*Right*) Magnification of each square. (*B–D*) High magnifications of BrdU-labeled Sox-2$^+$ but GFAP-negative ANPs (BrdU$^+$ANP; white arrowheads) and BrdU$^+$QNP (yellow arrowheads). The orthogonal projections are shown to confirm triple or double labeling throughout the cells. (Scale bars: *A*, 20 μm; *B–D*, 5 μm.)

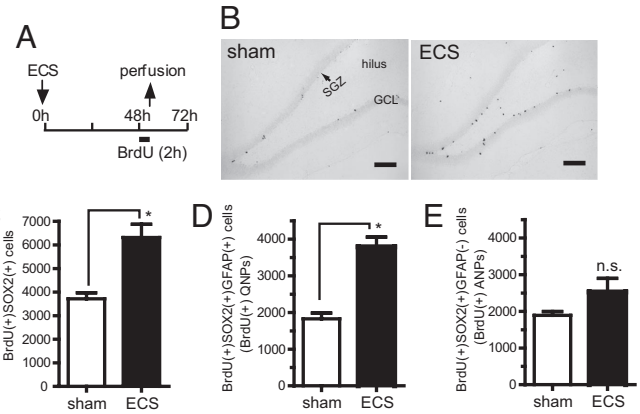

Fig. 2. ECS increases the proliferation of QNPs 2 h after BrdU labeling. (*A*) Experimental schema. Rats received injections of BrdU 48 h after sham or a single ECS and were killed 2 h later. (*B*) Representative coronal sections through the GCL with BrdU-labeled cells are shown from sham and single ECS. (Scale bars: 250 μm.) (*C–E*) Quantification of BrdU$^+$ and Sox-2$^+$ cells (*C*); BrdU$^+$, Sox-2$^+$, and GFAP$^+$ triple-labeled (BrdU$^+$QNP) cells (*D*); and BrdU$^+$, Sox-2$^+$, but GFAP-negative (BrdU$^+$ANP) cells (*E*) in SGZ of hippocampus after a single ECS compared with sham-handled controls. Data are shown as the means ± SEM, $n = 6$ for each group; *, $P < 0.05$; n.s., $P > 0.05$.

BrdU$^+$ANPs in SGZ, in some cases adjacent to BrdU$^+$QNPs, whereas others formed cell clusters (Fig. 1 *B* and *D*). The ratio of BrdU$^+$ cells among total ANPs was >50%, suggesting higher mitotic activity of this subclass (Fig. S2*A*). When we examined the ratio of QNPs to ANPs, >80% of Sox-2$^+$ cells were characterized as QNPs (GFAP$^+$) in rat SGZ (Fig. S2*B*). Because of the high ratio of QNPs, the actual number of BrdU$^+$QNP and BrdU$^+$ANP cells is almost identical despite the low mitotic activity of QNPs (Fig. S2*B*).

ECS Increases the Proliferation of QNPs. Previous studies have shown that all classes of antidepressants increase cell proliferation in the hippocampal SGZ (4, 7). A recent study using a nestin reporter mouse found that fluoxetine does not influence the division of QNPs, but increases the division of ANPs (13). Because ECS is the most efficacious stimulator of hippocampal cell proliferation, we investigated the effect of ECS on progenitor subclasses.

Our previous studies have demonstrated that the number of BrdU$^+$ cells doubles by 72 h after a single ECS but that there is no effect after 24 h (17). In the current work, we chose 48 h after ECS to inject BrdU to detect an early phase of progenitor cell proliferation. To isolate specifically the effect of ECS on the mitotic phase, rats were killed 2 h after BrdU injection. The number of BrdU$^+$ cells was significantly increased compared with that of sham-treated animals (sham, 3,762 ± 245; single ECS, 6,617 ± 648 BrdU$^+$ cells per SGZ; Fig. 2*B*). Most BrdU$^+$ cells within SGZ were Sox-2$^+$ in both the sham and ECS groups (sham, 98.7 ± 0.9%; single ECS, 95.9 ± 1.5%; Fig. 2*C*), indicating that the induction of QNP/ANP cell proliferation starts ≈2 days after a single ECS.

We further examined the expression of GFAP and Sox-2 in the BrdU$^+$ cells within SGZ and calculated the number of BrdU$^+$QNP and BrdU$^+$ANP cells. We found that ECS significantly increases the number of BrdU$^+$QNPs by ≈2-fold (Fig. 2*D*) and there is a tendency for an increase in the number of BrdU$^+$ANPs at this time point (Fig. 2*E*). In addition, the ratio of GFAP$^+$ cells among the BrdU$^+$Sox-2$^+$ population in the single-ECS group was significantly increased compared with that of the sham group (sham, 49.0 ± 1.2%; single ECS, 60.6 ± 2.7%), suggesting that a single ECS preferentially increases the proliferation of QNPs rather than ANPs at this early time point.

To characterize further the effects of ECS, the influence of single or repeated ECS treatment on QNP and ANP cells was determined 24 h after BrdU administration (Fig. 3*A*). A single ECS significantly increased the number of BrdU$^+$ cells in the SGZ by ≈1.7-fold, and seven daily ECS treatments resulted in a much greater induction of BrdU$^+$ cells of ≈5-fold (sham, 8,567 ± 490; single ECS, 14,492 ± 854; seven daily ECS, 41,832 ± 2,533 BrdU$^+$ cells per SGZ). Most BrdU$^+$ cells within SGZ were Sox-2$^+$ in all groups (sham, 99.2 ± 0.6%; single ECS, 96.6 ± 1.1%; seven daily ECS, 99.5 ± 0.5%), indicating that single and multiple ECS treatments increase the number of BrdU$^+$-proliferating QNP/ANP cells. Further analysis demonstrates that a single ECS significantly increased both BrdU$^+$QNP and BrdU$^+$ANP cells at the 24-h time point after BrdU (Fig. 3 *D* and *E*). This finding confirms the increase in QNPs observed 2 h after BrdU (Fig. 2*D*) and demonstrates that after a longer BrdU labeling time ECS also increases the subsequent proliferation of ANPs. Repeated ECS also increased the number of both BrdU$^+$ subclasses (Fig. 3 *D* and *E*). The induction of both BrdU$^+$QNPs and BrdU$^+$ANPs by repeated ECS was much higher than with a single ECS (≈4- to 5-fold relative to sham).

VEGF-Flk-1 Signaling Underlies ECS Induction of QNP Cell Proliferation. We have reported that ECS increases VEGF expression and that blockade of VEGF signaling blocks ECS induction of hippocampal cell proliferation (17), suggesting that VEGF could underlie increased QNP cell proliferation. To examine this possibility, we have determined the influence of VEGF and an inhibitor of VEGF-Flk-1 signaling on the proliferation of QNPs and ANPs.

Recombinant rat $VEGF_{164}$ was administered [10 ng/h, continuous i.v. infusion (i.c.v.), 72 h via s.c. osmotic minipump], and levels of BrdU$^+$ cells were determined (2 h after BrdU administration) (Fig. 4*A*). VEGF infusion significantly increased the number of BrdU$^+$ cells in the SGZ (control, 2,133 ± 111; VEGF, 3,642 ± 528). There was no significant difference in the ratio of Sox-2$^+$ cells to

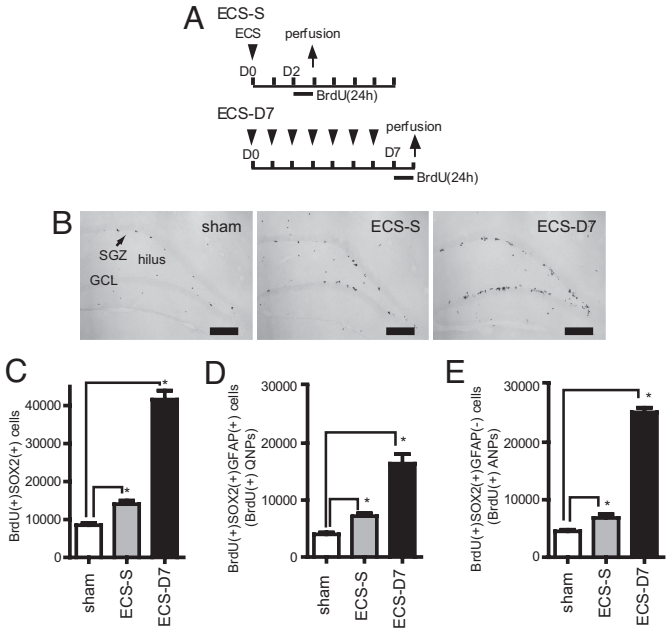

Fig. 3. ECS increases the proliferation of both QNPs and ANPs 24 h after BrdU labeling. (*A*) Experimental schema. Arrowheads show ECS treatment. ECS-S, single ECS; ECS-D7, multiple ECS, (seven times, once a day). Control group was sham-handled same as ECS-D7 group but without ECS. Rats received injections of BrdU after single or multiple ECS treatments, and all animals were killed 24 h later. (*B*) Representative coronal sections through the GCL with BrdU-labeled cells, from sham, ECS-S and ECS-D7. (Scale bars: 250 μm.) (*C–E*) Quantification of BrdU$^+$ and Sox-2$^+$cells (*C*); BrdU$^+$, Sox-2$^+$, and GFAP$^+$ triple-labeled (BrdU$^+$QNP) cells (*D*); and BrdU$^+$, Sox-2$^+$, but GFAP-negative (BrdU$^+$ANP) cells (*E*) in SGZ of hippocampus after a single or multiple ECS compared with sham-handled controls. Data are shown as the means ± SEM., $n = 6$ per group; *, $P < 0.05$; one-way ANOVA, followed by the post hoc Bonferroni test.

total BrdU$^+$ cells in SGZ (PBS, 98.7 ± 0.6%; VEGF, 98.9 ± 0.4%; Fig. 4*D*). Analysis of GFAP$^+$ cells demonstrates that VEGF increases BrdU$^+$QNPs by ≈2-fold (Fig. 4*E*) and BrdU$^+$ANPs by ≈1.5-fold (Fig. 4*F*) compared with vehicle.

The influence of low-dose irradiation exposure, which primarily affects rapidly proliferating cells in the SZG, was also examined. Two weeks after irradiation exposure, rats were infused with VEGF for 3 days and then administered BrdU (Fig. 4*A*). Consistent with previous studies (4–6), irradiation exposure significantly reduced the number of BrdU$^+$ cells (Fig. 4*D*). Irradiation did not influence number of BrdU$^+$QNPs but dramatically decreased the number of BrdU$^+$ANPs (Fig. 4 *E* and *F*). VEGF infusion significantly increased the number of BrdU$^+$QNP cells and increased the number of BrdU$^+$ANP after irradiation exposure. These results demonstrate that VEGF administration into brain stimulates QNP proliferation and thereby restores ANP proliferation.

We next investigated whether VEGF-Flk-1 receptor signaling is required for ECS induction of QNP and ANP proliferation. We used a small-molecule inhibitor of the Flk-1 receptor tyrosine kinase, SU5416. The inhibitory effect of this compound on ECS-induced cell proliferation in SGZ has been demonstrated (17). Vehicle or SU5416 was infused immediately before ECS and daily for 3 days after followed by administration of BrdU (Fig. 4*B*). SU5416 inhibited ECS induction of BrdU$^+$QNP and BrdU$^+$ANP cell populations (Fig. 4 *H* and *I*). The reason that ECS significantly increased the number of BrdU$^+$ANP cells in this experiment when there was less effect in the previous experiment (Fig. 2*C*) is likely a result of the time after treatment (72 h vs. 48 h, respectively).

To investigate further the primary cell target for VEGF administration, we examined the effect of VEGF infusion for 24 h on QNP

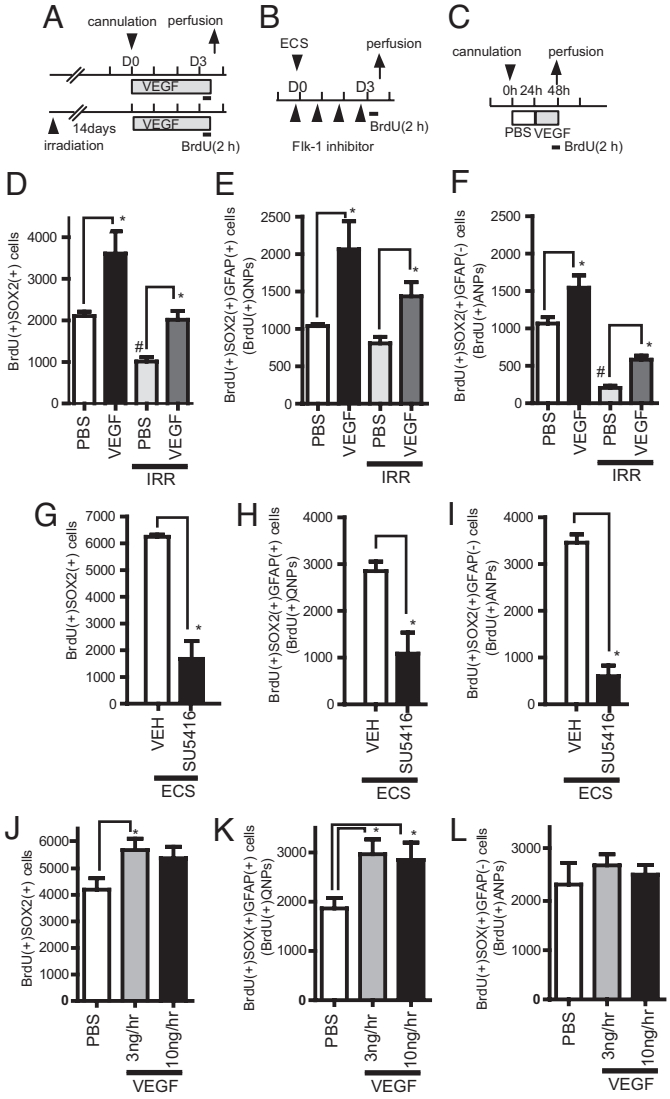

Fig. 4. Role of VEGF-Flk-1 signaling in the regulation of QNP and ANP proliferation in rat DG. (*A–C*) Experimental schema. (*A*) Recombinant rat VEGF$_{164}$ was infused i.c.v. for 3 days via osmotic minipump, with or without irradiation (IRR) exposure. (*B*) Flk-1 inhibitor SU5416 was delivered (i.c.v.) 30 min before ECS, followed by three daily infusions. (*C*) VEGF$_{164}$ was continuously infused (i.c.v.) for 24 h via osmotic minipump. All animals were injected with BrdU at the indicated time point and killed 2 h after injection. (*D–F*) VEGF increases the proliferation of both QNPs and ANPs with or without irradiation exposure. Note that irradiation exposure preferentially reduced proliferation of the ANP population. (*G–I*) VEGF-Flk-1 signaling mediates ECS-induced QNP and ANP proliferation. (*J–L*) VEGF administration for 24 h preferentially increases the proliferation of QNPs. VEH, vehicle. Data are shown as the means ± SEM, $n = 4–6$ per group; *, $P < 0.05$ compared with vehicle-infused controls. One-way ANOVA, followed by Bonferroni (*D–F* and *J*), *t* test (*F–H*) or Kruskal–Wallis followed by Dunn's multiple comparison post hoc test (*K*) were used. #, $P < 0.05$; compared with nonirradiation controls; two-way ANOVA, followed by Bonferroni post hoc test (*B–D*).

and ANP proliferation. To avoid the influence of the cannulation and anesthesia, PBS was infused for 24 h before VEGF administration (Fig. 4*C*). Acute VEGF administration preferentially increased the proliferation of QNPs at the same dose tested above (10 ng/h) and at a lower dose (3 ng/h) (Fig. 4 *J–L*).

Expression of VEGF and Flk-1 in Rat Hippocampus. We have shown that ECS increases the expression of VEGF mRNA in rat hip-

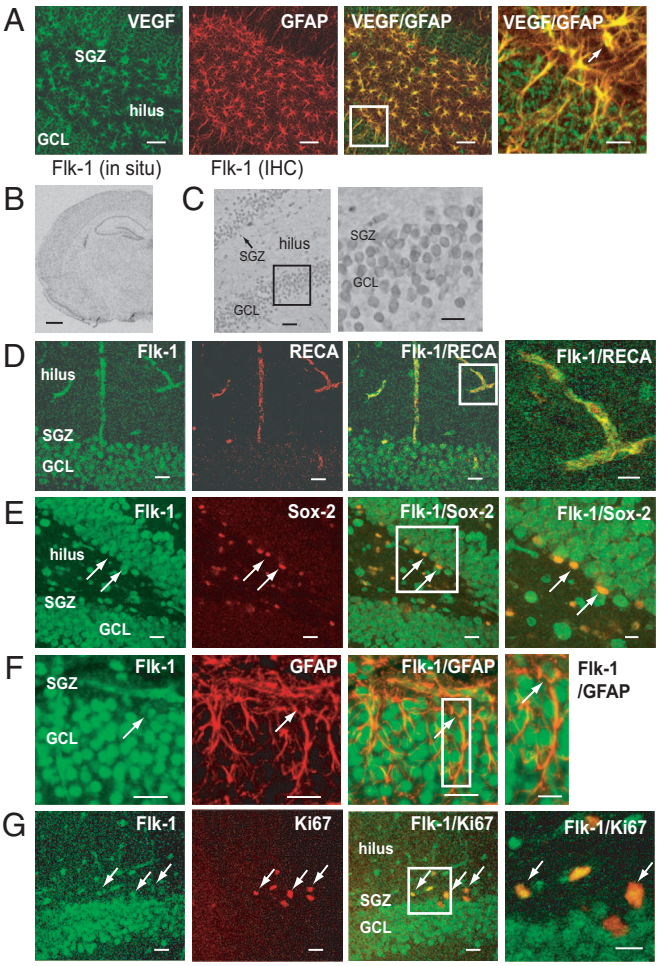

Fig. 5. Expression of VEGF and Flk-1 in rat hippocampus. (*A*) (*Left* and *Center*) VEGF (green) and GFAP (red) immunoreactivity (IR) in rat hilus and GCL. VEGF-IR in hilus is mainly colocalized with GFAP. (Scale bars: 50 μm.) (*Right*) VEGF expression in the GCL shows a punctuate appearance. (Scale bar: 25 μm.) (*B* and *C*) Representative autoradiogram of Flk-1 mRNA expression (*B*). (Scale bar: 1 mm.) and Flk-1-IR (*C*). [Scale bars: 20 μm (*Right*) and 10 μm (*Left*).] (*D–G*) Confocal images of Flk-1-IR (green) and (*D*) the endothelial marker RECA (red), (*E*) the neural stem-like and progenitor cell marker Sox-2, (*F*) the neural stem-like or astrocytic marker GFAP (red), or (*G*) the cell proliferation marker Ki67 (red), and merged images (*Right*). Arrows in *E* show colocalization of Flk-1-IR and Sox-2-IR in SGZ. Arrow in *F* shows an Flk-1-expressing cell in the SGZ, which has a process through the DG that is visualized with GFAP. Arrows in *G* show colocalization of Flk-1-IR and Ki67-IR in the SGZ. [Scale bars: 20 μm except magnified panels (*Right*, 10 μm).]

pocampus (17). Here, we show that VEGF immunoreactivity (IR) in SGZ and hilus is colocalized with GFAP-IR (Fig. 5*A*), indicating that VEGF is expressed in QNPs and astrocytes. In addition, a punctate expression pattern was observed on the somata of the dentate gyrus granule cells (GFAP-negative cells), consistent with the expression of VEGF mRNA in this population of cells (17).

Flk-1 mRNA was expressed in the granule and pyramidal cell layers of the hippocampus in naive rat brain (Fig. 5*B*) and was not changed by single ECS (2, 6, or 24 h after ECS; data not shown). Flk-1 IR was also observed in the granule and pyramidal cell layers of the hippocampus (Fig. 5*C* and data not shown). Flk-1 IR was colocalized with an endothelial cell marker, RECA (Fig. 5*D*), and a mature neuronal marker, NeuN (data not shown). In the SGZ, Flk-1 IR was colocalized with a QNP/ANP marker, Sox-2 (Fig. 5*E*). Flk-1 IR was surrounded by GFAP-IR (Fig. 5*F*) in a subpopulation of cells of SGZ, indicating Flk-1 is expressed in QNPs. In addition,

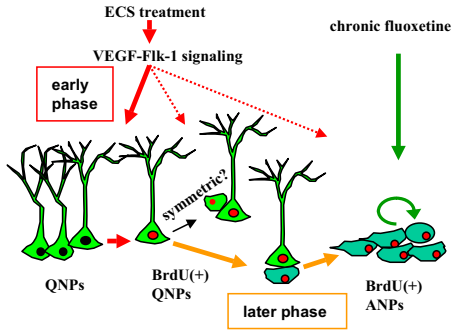

Fig. 6. Model of ECS induction of QNPs. Single or repeated ECS increases VEGF expression and signaling, thereby leading to induction of QNP cell proliferation. The induction of ANP cell proliferation may occur via asymmetric division of QNPs, or via direct effects of VEGF-Flk-1 signaling on ANP cells. This contrasts with the induction of ANP but not QNP cell proliferation in response to chronic fluoxetine administration.

many mitotic cells labeled with the cell cycle marker Ki67 were also positive for Flk-1 IR (Fig. 5*G*). These expression studies suggest that ECS induction of VEGF in the SGZ, either granule cells or GFAP$^+$ cells, stimulates QNP proliferation via Flk-1 signaling located on these cells.

Discussion

In the current work, we show that the primary cell target for ECS is induction of QNP cell proliferation within SGZ of adult hippocampus. This differentiates ECS from the chemical antidepressant fluoxetine, which increases the proliferation of ANP but not QNP cells (13) and accounts for the superior efficacy of ECS induction of hippocampal cell proliferation and neurogenesis (7). Because BrdU labels in the S phase of the cell cycle and most BrdU-labeled cells do not enter the M phase at the 2-h time point examined, the results demonstrate that ECS shifts QNPs from a quiescent or resting phase to a mitotic phase. When cells are labeled with BrdU for a longer time (24 h), both QNP and ANP proliferation are significantly increased after a single ECS. Increased ANP proliferation could result from asymmetric division of QNPs by ECS, giving rise to one QNP and one ANP and then subsequent symmetric division and amplification of the daughter ANPs (18). It is also possible that ECS directly activates ANP proliferation, although it is difficult to explain why this would not be observed at the 2-h time point. It is also notable that at the 24-h BrdU labeling time point we observe some BrdU$^+$QNP clusters that are GFAP$^+$ but do not have processes that extend across the granule cell layer (E.S.-N. and R.S.D., unpublished data). This observation suggests that ECS might stimulate "symmetric-like" division of QNPs (producing two daughter QNP cells), although additional work is required to test this possibility. Fig. 6 shows a model of ECS and VEGF regulation of the proliferation of QNPs and ANPs. Yet another possibility is that QNPs are derived from ANP cell proliferation, a hypothesis proposed in a recent article (19).

In the current work, the ratio of BrdU$^+$QNPs relative to the total number of BrdU$^+$Sox-2$^+$ progenitor cells in rat hippocampus was $\approx$50% at the 2-h time point. Because nearly 90% of Sox-2$^+$ cells are classified as QNPs, the actual numbers of BrdU$^+$QNPs and BrdU$^+$ANPs are similar despite low mitotic activity of QNPs. A previous study using mice reported a similar percentage of GFAP$^+$/BrdU$^+$ cells (designated B cells) (11), whereas other studies using nestin-GFP transgenic mice reported only 6% of nestin-GFP$^+$/BrdU$^+$ cells with the presence of processes (designated type 1 cells) (12) or using Sox2-GFP transgenic mice that all dividing cells were nonradial glia (19). The study using nestin-GFP mice also showed that only 61% of BrdU$^+$ cells are nestin-GFP$^+$. The current study showed that >95% of BrdU$^+$ cells are Sox-2$^+$ cells. In addition, it

has been reported that ≈40% of Sox-2$^+$ cells in SGZ do not overlap with nestin-GFP$^+$ in mouse SGZ (16). Although both Sox-2 and nestin are considered markers for neural stem/progenitor cells, it would be interesting to analyze the character of Sox-2$^+$/nestin$^-$/BrdU$^+$ cell population.

VEGF is reported to stimulate adult neurogenesis *in vivo* (20, 21) and proliferation of brain-derived neural stem/progenitor cells *in vitro* (22, 23). We have reported that VEGF-Flk-1 signaling underlies ECS induction of hippocampal cell proliferation (17) and importantly, rescues hippocampal cell proliferation after irradiation exposure (24). The current study extends this work, demonstrating that VEGF is sufficient to stimulate QNP proliferation in intact and irradiated animals and that VEGF-Flk-1 signaling is required for ECS induction of QNPs. The induction of ANP proliferation in response to VEGF administration for 3 days could result from asymmetric division of QNPs, as discussed for ECS.

We found that irradiation dramatically decreases the number of BrdU$^+$ANPs but not BrdU$^+$QNPs (Fig. 4 *C* and *D*), whereas a recent study found that the total number of ANPs and QNPs is reduced shortly after irradiation (25). A possible explanation for this difference is the time of analysis after irradiation (2 weeks for the current study vs. hours for the recent report). It is possible that QNP proliferation is initially sensitive to irradiation but that the proliferative activity can recover at later time points, whereas ANP proliferation is essentially eliminated because of the high rate proliferation and microenvironmental changes after irradiation (26).

Previous studies have reported that pathological stimuli, such as kainite- or pilocarpine-induced seizures and cortical ischemic infarcts, also stimulate proliferation of QNPs in addition to ANPs and a doublecortin-positive cell population (type 3 cells) (27–29). One of the differences between kainite-induced seizure and ECS is that kainate-induced seizures also result in neurotoxicity and cell loss accompanying neuronal apoptosis (30), whereas ECS does not result in apoptosis or cell damage (31). The short duration and reduced severity of ECS could be sufficient to induce VEGF-mediated QNP proliferation without the cell loss or damage produced by kainate. Based on the results of the current work, it would be interesting to examine the involvement of VEGF-Flk-1 signaling in neurotoxin- or ischemia-induced QNP proliferation. The current work demonstrates that acute ECS preferentially induces proliferation of QNPs and that ECS-induced QNP and subsequent ANP proliferation is mediated by VEGF-Flk-1 signaling. We have reported that induction of cell proliferation in the SGZ by chemical antidepressants (presumably ANPs) also requires VEGF-Flk-1 signaling (17). These results indicate that VEGF influences both QNP and ANP cell proliferation, and the treatment specific responses could be caused by temporal and/or dose-dependent effects of VEGF on each cell type. In the current work we found that acute VEGF administration (24 h) preferentially increases the proliferation of QNPs, suggesting that ECS induction of QNP proliferation is caused by relatively fast and robust induction of VEGF. In contrast, the induction of VEGF in response to chemical antidepressants requires chronic (2 weeks) treatment, and this slower onset and lower, but continuous induction of VEGF levels, may support ANP, but not QNP proliferation (17). Additional studies will be required to characterize further the time- and dose-dependent effects of VEGF on the proliferation of ANPs in SGZ of hippocampus.

Taken together, the results demonstrate that ECS stimulates the expression and function of VEGF-Flk-1 signaling within the DG, which leads to the stimulation of QNP and then ANP proliferation. The ability of ECS to induce a high level of VEGF expression and to stimulate QNP proliferation underlies the greater induction of neurogenesis by ECS in the adult hippocampus relative to chemical antidepressants (7). Because a single ECS can induce QNP proliferation and net neurogenesis (7, 31), ECS results in a more rapid induction of neurogenesis relative to chemical antidepressant treatments. The relationship between ECS induction of QNP proliferation/neurogenesis and the superior therapeutic efficacy of ECT for the treatment of mood disorders, including refractory depression, remains unknown. However, it is notable that ECS restores a therapeutic response to chemical antidepressants in patients that were previously nonresponsive (32), raising the possibility that ECT could activate QNPs and subsequent daughter ANPs that could then respond to chemical antidepressant treatments. The results of the current work could be useful in identifying agents that stimulate VEGF and QNP proliferation and could possibly have superior therapeutic efficacy, similar to ECS.

Materials and Methods

Animals. Male Sprague–Dawley rats (Charles River Laboratories) weighing 175–250 g were pair-housed and maintained in standard conditions with a 12-h light/dark cycle and ad libitum access to food and water. Animal use and procedures were in accordance with the National Institute of Health guidelines and approved by the Yale University School of Medicine Institutional Animal Care and Use Committees.

ECS Treatment. ECS was administered via ear clip electrodes with a pulse generator (Ugo Basile) (55–60 mA, 0.5-s duration, 100-Hz frequency) to induce a generalized grand mal seizure lasting for <15 s. Acute animals received one ECS, and chronic animals received seven ECS (one per day). Sham groups were handled identically but received no shock.

Irradiation Procedure. Anesthetized rats were placed under a Stabilipan (Siemens) therapeutic unit (2.15 Gy/min at 250 kV) and subjected to a single 10-Gy irradiation dose directed at the whole cranium (24). The rest of the head and body were protected with lead shielding. VEGF i.c.v. infusion was started 2 weeks after irradiation.

BrdU Administration. For labeling dividing cells during S phase of mitosis, rats were administered BrdU (150 mg/kg, i.p.; Sigma) at indicated time points and perfused with PBS and 10% formalin 2 h or 24 h after the BrdU injection.

Surgical Procedures. Rats were anesthetized with ketamine (80 mg/kg, i.m.) and xylazine (6 mg/kg, i.m.), and stereotaxic surgeries were performed as described in ref. 17. Briefly, a guide cannula was implanted into lateral ventricle (coordinates from bregma: −0.9 anterior/posterior, −1.5 mediolateral, −3.3 dorsal/ventral from dura). VEGF receptor Flk-1 tyrosine kinase inhibitor, SU5416 (4 mM; Sigma) was infused in 1-μl volume i.c.v. through the infusion cannula (0.25 μl/min). Recombinant VEGF$_{164}$ (10 ng/μl or 3 ng/μl; Sigma) or PBS was delivered i.c.v. via an implanted (s.c.) microosmotic pump (Durect) at a rate of 1 μl/h for 3 days or 24 h.

Immunohistochemistry. Free-floating sections were used for detection of BrdU-labeled cells, and triple immunostaining was performed as described in ref. 33. For triple labeling to characterize the phenotype of BrdU-labeled cells, mouse anti-BrdU (1:200; BD Transduction Laboratories), rabbit anti-GFAP (AB5804, 1:1,000; Chemicon), and goat anti-Sox-2 (Y-17, 1:200; Santa Cruz Biotechnology) were used as primary antibodies. Fluorescent-labeled antibodies (Alexa Fluor 488, 546, and 633, 1:300; Molecular Probes) were used as secondary antibodies. Anti-VEGF (Ab-4, 1:300, Calbiochem) and anti-GFAP double immunostaining was performed essentially as described for the triple immunostaining without 50% formamide and 2 N HCl treatment. For Flk-1 immunostaining, fresh-frozen sections (14-μm thick) were cut and fixed in either 4% paraformaldehyde (for double staining with anti-GFAP, anti-Sox-2 or anti-Ki67, 20 min, 4°C) or acetone and methanol (for double staining with anti-RECA, 10 min, −20°C, each fixation). Sections were washed and blocked with 5% horse serum followed by incubation in primary antibodies. Sections were washed before incubation with fluorescent- or peroxidase-labeled secondary antibodies. Rabbit anti-Flk-1 (sc-504, 1:100; Santa Cruz Biotechnology), mouse anti-rat RECA-1 (1:20; Serotec), mouse anti-Ki67 (MM1, 1:20; Novocastra), goat anti-Sox-2 (Y-17, 1:200) and mouse anti-GFAP (GA-5, 1:2,000; Sigma) were used as primary antibodies.

Quantitation of BrdU Single- and Triple-Labeled Cells. For single BrdU-labeled cell quantification, a modified unbiased stereological procedure was used as described in ref. 7. Sections were coded to ensure that analysis was performed by a blind observer, and BrdU$^+$ cells were counted in the SGZ of the hippocampus on a light microscope (Olympus BX-60). Cells were included in SGZ counts if the cell was in or touching the SGZ (the layer of cells on the border of the GCL and hilus). If a cell was more than two cell diameters from the GCL, that cell was excluded.

Every sixth 40-μm-thick section was counted throughout the hippocampus, and the sum was multiplied by 6 to provide an estimate of the total number of $BrdU^+$ cells in the entire region. For the phenotypic analysis of BrdU-labeled cells, slices were analyzed on a confocal microscope (Zeiss, LSM510meta) and Z-sectioning (1-μm steps, 10–15 sections per slice) to determine whether BrdU-labeled cells were colabeled with Sox-2 and GFAP. At least 50 $BrdU^+$ cells per animal were analyzed. We have used this approach in previous studies for the phenotype of BrdU-labeled cells (7, 17, 33).

Flk-1 mRNA Detection. *In situ* hybridization was performed by using radiolabeled riboprobe as described in ref. 34. Flk-1 template probe (nucleotides 1774–2061 of rat Flk-1 cDNA, GenBank accession number U93306) was generated by PCR with gene-specific primers, verified by sequencing, and used to produce radiolabeled riboprobe with a T7-based *in vitro* transcription kit (Megashortscript; Ambion). Coronal brain sections (14-μm thick) were cut on a cryostat, mounted onto slides, fixed in 4% paraformaldehyde, acetylated, and dehydrated before hybridization. Sections were hybridized with the riboprobe (2×10^6 cpm per section) for 18 h at 55°C. Slides were washed, dried, and exposed to Biomax film (Kodak).

Statistical Analyses. All data are presented as means ± SEM, and experiments with two groups were compared with unpaired Student's *t* test, whereas experiments with three or more groups were subjected to one-way or two-way ANOVA, followed by the Bonferroni post hoc test. Kruskal–Wallis followed by Dunn's multiple comparison tests for nonparametric data were used (Fig. 4*K*). Significance marks in figures are based on results from *t* test or Bonferroni or Dunn's post hoc test. Statistical significance was set at $P < 0.05$.

ACKNOWLEDGMENTS. We thank Dr. Ja Wook Koo and Ms. Pingxing Xie for helpful discussion and technical assistance. This work was supported by U.S. Public Health Service Grants MH25642 and MH45481, by the Connecticut Mental Health Center, and by a Uehara Memorial Foundation fellowship (to E.S.-N.).

1. Janicak PG, *et al.* (1985) Efficacy of ECT: A meta-analysis. *Am J Psychiatry* 142:297–302.
2. UK ECT Review Group (2003) Efficacy and safety of electroconvulsive therapy in depressive disorders: A systemic review and meta-analysis. *Lancet* 361:799–808.
3. Pagnin D, de Queiroz V, Pini S, Cassano GB (2004) Efficacy of ECT in depression: A meta-analytic review. *J ECT* 20:13–20.
4. Santarelli L, *et al.* (2003) Requirement of hippocampal neurogenesis for the behavioral effects of antidepressants. *Science* 301:805–809.
5. Jiang W, *et al.* (2005) Cannabinoids promote embryonic and adult hippocampus neurogenesis and produce anxiolytic- and antidepressant-like effects. *J Clin Invest* 115:3104–3116.
6. Airan RD, *et al.* (2007) High-speed imaging reveals neurophysiological links to behavior in an animal model of depression. *Science* 317:819–823.
7. Malberg JE, Eisch AJ, Nestler EJ, Duman RS (2000) Chronic antidepressant treatment increases neurogenesis in adult rat hippocampus. *J Neurosci* 20:9104–9110.
8. Nakagawa S, *et al.* (2002) Regulation of neurogenesis in adult mouse hippocampus by cAMP and the cAMP response element-binding protein. *J Neurosci* 22:3673–3682.
9. Perera TD, *et al.* (2007) Antidepressant-induced neurogenesis in the hippocampus of adult nonhuman primates. *J Neurosci* 27:4894–4901.
10. Wang JW, *et al.* (2008) Chronic fluoxetine stimulates maturation and synaptic plasticity of adult-born hippocampal granule cells. *J Neurosci* 28:1374–1384.
11. Seri B, Garcia-Verdugo JM, McEwen BS, Alvarez-Buylla A (2001) Astrocytes give rise to new neurons in the adult mammalian hippocampus. *J Neurosci* 21:7153–7160.
12. Filippov V, *et al.* (2003) Subpopulation of nestin-expressing progenitor cells in the adult murine hippocampus shows electrophysiological and morphological characteristics of astrocytes. *Mol Cell Neurosci* 23:373–382.
13. Encinas JM, Vaahtokari A, Enikolopov G (2006) Fluoxetine targets early progenitor cells in the adult brain. *Proc Natl Acad Sci USA* 103:8233–8238.
14. Komitova M, Eriksson PS (2004) Sox-2 is expressed by neural progenitors and astroglia in the adult rat brain. *Neurosci Lett* 369:24–27.
15. Hattiangady B, Shetty AK (2008) Aging does not alter the number or phenotype of putative stem/progenitor cells in the neurogenic region of the hippocampus. *Neurobiol Aging* 29:129–147.
16. Steiner B, *et al.* (2006) Type 2 cells as link between glial and neuronal lineage in adult hippocampal neurogenesis. *Glia* 54:805–814.
17. Warner-Schmidt JL, Duman RS (2007) VEGF is an essential mediator of the neurogenic and behavioral actions of antidepressants. *Proc Natl Acad Sci USA* 104:4647–4652.
18. Kempermann G (2006) *Adult Neurogenesis, Stem Cells and Neuronal Development in the Adult Brain* (Oxford, New York), pp 168–191.
19. Suh H, *et al.* (2007) *In vivo* fate analysis reveals the multipotent and self-renewal capacities of $Sox\text{-}2^+$ neural stem cells in the adult hippocampus. *Cell Stem Cell* 1:515–528.
20. Jin K, *et al.* (2002) Vascular endothelial growth factor (VEGF) stimulates neurogenesis *in vitro* and *in vivo*. *Proc Natl Acad Sci USA* 99:11946–11950.
21. Cao L, *et al.* (2004) VEGF links hippocampal activity with neurogenesis, learning and memory. *Nat Genet* 36:827–835.
22. Fabel K, *et al.* (2003) VEGF is necessary for exercise-induced adult hippocampal neurogenesis. *Eur J Neurosci* 18:2803–2812.
23. Wada T, *et al.* (2006) Vascular endothelial growth factor directly inhibits primitive neural stem cell survival but promotes definitive neural stem cell survival. *J Neurosci* 26:6803–6812.
24. Warner-Schmidt JL, Madsen TM, Duman RS (2008) Electroconvulsive seizure restores neurogenesis and hippocampus-dependent fear memory after disruption by irradiation. *Eur J Neurosci* 27:1485–1493.
25. Encinas JM, Enikolopov G (2008) Identifying and quantitating neural stem and progenitor cells in the adult brain. *Methods Cell Biol* 85:243–272.
26. Monje ML, Mizumatsu S, Fike JR, Palmer TD (2002) Irradiation induces neural precursor cell dysfunction. *Nat Med* 8:955–962.
27. Huttmann K, *et al.* (2003) Seizures preferentially stimulate proliferation of radial glia-like astrocytes in the adult dentate gyrus: Functional and immunocytochemical analysis. *Eur J Neurosci* 18:2769–2778.
28. Kunze A, *et al.* (2006) Proliferative response of distinct hippocampal progenitor cell populations after cortical infarcts in the adult brain. *Neurobiol Dis* 21:324–332.
29. Shapiro LA, Figueroa-Aragon S, Ribak CE (2007) Newly generated granule cells show rapid neuroplastic changes in the adult rat dentate gyrus during the first five days after pilocarpine-induced seizures. *Eur J Neurosci* 26:583–592.
30. Bengzon J, *et al.* (1997) Apoptosis and proliferation of dentate gyrus neurons after single and intermittent limbic seizures. *Proc Natl Acad Sci USA* 94:10432–10437.
31. Madsen TM, *et al.* (2000) Increased neurogenesis in a model of electroconvulsive therapy *Biol Psychiatry* 47:1043–1049.
32. van den Broek WW, *et al.* (2006) Imipramine is effective in preventing relapse in electroconvulsive therapy-responsive depressed inpatients with prior pharmacotherapy treatment failure: A randomized, placebo-controlled trial. *J Clin Psychiatry* 67:263–268.
33. Madsen TM, Yeh DD, Valentine GW, Duman RS (2005) Electroconvulsive seizure treatment increases cell proliferation in rat frontal cortex. *Neuropsychopharmacology* 30:27–34.
34. Newton SS, *et al.* (2003) Gene profile of electroconvulsive seizures: Induction of neurotrophic and angiogenic factors. *J Neurosci* 23:10841–10851.